Observation of the 1154.9 nm transition of antiprotonic helium

T. Kobayashi[1], D. Barna[1,2], R. S. Hayano[1], Y. Murakami[1], K. Todoroki[1], H. Yamada[1], A. Dax[3], L. Venturelli[4,5], N. Zurlo[4,5], D. Horváth[2,6], H. Aghai-Khozani[7,8], A. Sótér[7], and M. Hori[7,1]

[1]Department of Physics, University of Tokyo, Hongo, Bunkyo-ku 113-0033, Japan
[2]Institute for Particle and Nuclear Physics, Wigner Research Centre for Physics, Hungarian Academy of Sciences, P.O.Box 49, Budapest, 1525, Hungary
[3]Paul Scherrer Institute, 5232 Villigen-PSI, Switzerland
[4]Dipartimento di Ingegneria dell ' Informazione, Universitá di Brescia, 25123 Brescia, Italy
[5]INFN, Gruppo Collegato di Brescia, 25133 Brescia, Italy
[6]Institute of Nuclear Research, H-4001 Debrecen, Hungary
[7]Max-Planck-Institut für Quantenoptik, Hans-Kopfermann-Strasse 1, D85748 Garching, Germany
[8]CERN, CH-1211 Geneva 23, Switzerland

E-mail: `tkobayashi@nucl.phys.s.u-tokyo.ac.jp`

Abstract. The resonance transition $(n, l) = (40, 36) \rightarrow (41, 35)$ of the antiprotonic helium ($\overline{\mathrm{p}}^4\mathrm{He}^+$) isotope at a wavelength of 1154.9 nm was detected by laser spectroscopy. The population of $\overline{\mathrm{p}}^4\mathrm{He}^+$ occupying the resonance parent state $(40, 36)$ was found to decay at a rate of 0.45 ± 0.04 $\mu\mathrm{s}^{-1}$, which agreed with the theoretical radiative rate of this state. This implied that very few long-lived $\overline{\mathrm{p}}^4\mathrm{He}^+$ are formed in the higher-lying states with principal quantum number $n \geq 41$, in agreement with the results of previous experiments.

The antiprotonic helium atom $\overline{\mathrm{p}}\mathrm{He}^+$ is a Coulomb three-body system consisting of an antiproton, an electron in the ground state, and a helium nucleus [1,2]. The antiproton occupies a Rydberg state with large principal ($n \sim 38$) and orbital angular momentum ($l \sim n-1$) quantum numbers (Figure 1). These states are metastable, i.e., they have microsecond-scale lifetimes against antiproton annihilations. The atomic transition frequencies of $\overline{\mathrm{p}}\mathrm{He}^+$ involving laser excitations of the antiproton between various (n,l) states have been recently measured by laser spectroscopy with a fractional precision of $(2.3-5)\times 10^{-9}$ [3]. Comparisons between the measured frequencies and three-body QED calculations have yielded a value for the antiproton-to-electron mass ratio [3]. More recently, the data were used to establish limits on the fifth fundamental force [4].

This paper presents the observation of the transition $(n,l)=(40,36)\rightarrow(41,35)$ of the antiprotonic helium isotope $\overline{\mathrm{p}}^4\mathrm{He}^+$ at a wavelength of $\lambda = 1154.9$ nm (Figure 1). This transition wavelength is longer than that of any $\overline{\mathrm{p}}\mathrm{He}^+$ resonance studied so far. These transitions in the highly excited $n \geq 40$ region are not particularly suitable for precision laser spectroscopy, since the intensities of the resonance signals are relatively weak, and the transition frequencies are low, in the near infrared region. Additionally, the states involved in the laser transition are often strongly perturbed by collisions with other helium atoms. Nevertheless, these transitions do provide important information about the formation process of these atoms, since a laser resonance signal can only be detected if a significant number of the $\overline{\mathrm{p}}\mathrm{He}^+$ atoms were formed in the resonance parent state, e.g., $(n,l)=(40,36)$ for the 1154.9 nm transition. Most of the earlier studies on $\overline{\mathrm{p}}\mathrm{He}^+$ concentrated on the lower-lying $n \leq 39$ states, whereas a small fraction of antiprotons that occupy some $n=40$ states have been previously detected by measuring some other laser transitions, e.g., $(n,l)=(40,35)\rightarrow(39,34)$ [5,6].

The $\overline{\mathrm{p}}\mathrm{He}^+$ atoms are produced by colliding antiprotons with helium atoms at electron-volt energies,

$$\overline{\mathrm{p}} + \mathrm{He} \rightarrow (\overline{\mathrm{p}}\mathrm{He}^+)_{n,l} + \mathrm{e}^-. \tag{1}$$

Laser spectroscopic studies of numerous $\overline{\mathrm{p}}\mathrm{He}^+$ transitions have mapped out the distributions of $\overline{\mathrm{p}}\mathrm{He}^+$ occupying these metastable states (n,l) at the formation of the atom [6, 7]. These studies have revealed the largest population in the $n=38$ region. Among the theoretical studies on the capture process of antiprotons in helium atoms [8–13], many showed that capture is most likely to occur into $\overline{\mathrm{p}}^4\mathrm{He}^+$ states with principal quantum numbers of around,

$$n_0 = \sqrt{M^*_{\overline{\mathrm{p}}}/m_{\mathrm{e}}} = 38.3, \tag{2}$$

where $M^*_{\overline{\mathrm{p}}}$ denotes the reduced mass of the $\overline{\mathrm{p}}-^4\mathrm{He}$ system. Eq. (2) is derived from the assumption [14, 15] that the radius and binding energy of the antiproton are the same as those of the displaced electron in the $1s$ state. This hypothesis is supported by the results of the previous experiments described above.

The $\overline{\mathrm{p}}\mathrm{He}^+$ atoms slowly cascade down to lower states via radiative decays $\Delta n = \Delta l = -1$, i.e., keeping the vibrational quantum number $v = n-l-1$ [1,2] constant.

They finally reach short-lived states that have picosecond-to-nanosecond-scale lifetimes against Auger emission of the electron,

$$\overline{\mathrm{p}}\mathrm{He}^{+} \rightarrow \overline{\mathrm{p}}\mathrm{He}^{2+} + \mathrm{e}^{-}. \tag{3}$$

The $\overline{\mathrm{p}}\mathrm{He}^{2+}$ ions, which remain after the Auger decay, are rapidly destroyed by collisions with helium atoms (see the caption of Figure 1). The cascade process has been studied by measuring time evolutions of the populations in many states with $n \leq 40$ [6, 7]. Here we similarly study the population in the state $(40, 36)$ in the $v = 3$ cascade.

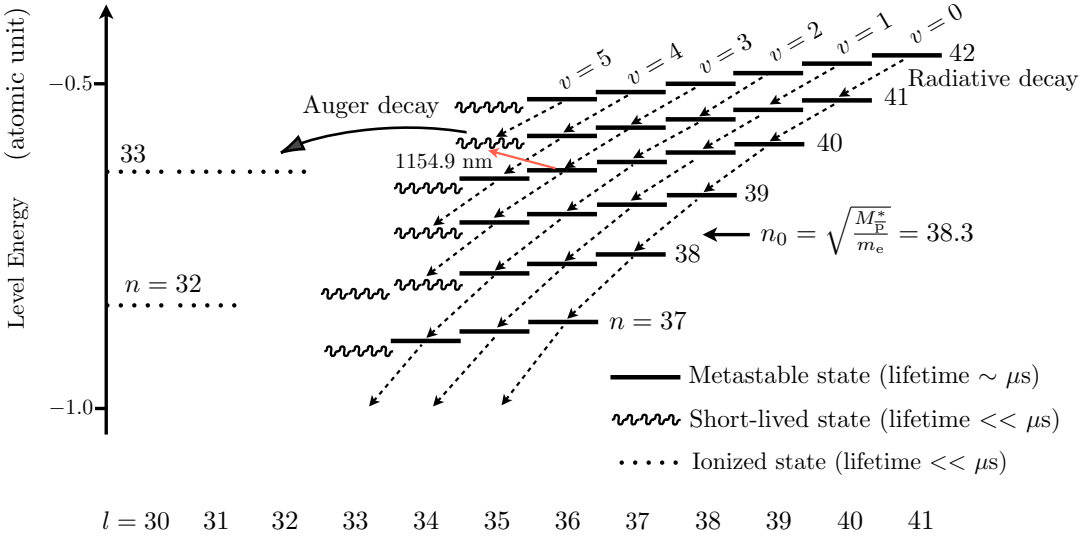

Figure 1. Energy diagram of the $\overline{\mathrm{p}}^{4}\mathrm{He}^{+}$ atom. The 1154.9 nm transition observed in this work is indicated with a solid red arrow. The ionized l-states with the same n are degenerate so that collisional Stark effect mix the large-l states with the low-l states (the s, p and d states) at large n, resulting in a rapid annihilation of the antiproton in the helium nucleus. Dashed arrows show radiative decays with microsecond-scale lifetimes.

The present experiment was carried out at the Antiproton Decelerator (AD) of CERN. The experimental setup was similar to that of Ref. [5], and so we here restrict ourselves to a short description. A pulsed beam containing $(2-3) \times 10^{7}$ antiprotons with a momentum of 100 MeV/c, a pulse length of $200-300$ ns, and a repetition rate of 0.01 Hz was extracted from the AD. We stopped the antiprotons in a cryogenic helium gas target [16] to produce the $\overline{\mathrm{p}}\mathrm{He}^{+}$ atoms. The profile of the antiproton beam some 2 m upstream of the target was measured by secondary electron emission chambers [17], and used to steer the beam into the target. The target contained ^{4}He gas at a temperature of $5-6$ K and a pressure of 60 kPa. A pulsed laser induced the atomic transition between the metastable state $(40, 36)$ and a state $(41, 35)$ with a short Auger lifetime. The $\overline{\mathrm{p}}\mathrm{He}^{2+}$ ions remaining after Auger decay were destroyed by collisions within picoseconds. The

charged pions emerging from the resulting antiproton annihilations were detected by a Cherenkov counter [18]. A high laser fluence of 1 mJ/cm^2 was used, which saturated the transition. This was needed since the number of $\overline{\mathrm{p}}\mathrm{He}^+$ populating $(n, l) = (40, 36)$ was relatively small [6], and so the resonance signal was weak. The timing of the laser was varied between $t = 0.5 - 8$ μs after the arrival of the antiproton pulse. A photodiode was located near the target to measure the temporal profile of the laser pulse.

A stimulated first-order Raman scattering process in a H_2 gas cell was utilized to generate a 7 ns long laser pulse with a wavelength of 1154.9 nm, a power of 4.5 mJ, and a diameter of 2 cm. The timing jitter and power fluctuation of the laser was around 10 ns and 10%, respectively. The pump beam for the Raman conversion was provided by an injection-seeded titanium sapphire (Ti:S) laser [19], which produced a light pulse of wavelength λ =780.4 nm. This beam was allowed to pass through a 3 m long Raman gas cell filled with H_2 gas at room temperature and a pressure of 600 kPa. The frequency of the resulting collinear Stokes beam ν_{S} was determined from the relationship $\nu_{\mathrm{S}} = \nu_{\mathrm{Ti:S}} - \nu_{\mathrm{R}}$, where $\nu_{\mathrm{Ti:S}}$ is the frequency of the Ti:S pump laser and $\nu_{\mathrm{R}} = 124\,570.6 \pm 0.5$ GHz the vibrational $Q(1)$ transition frequency of H_2 [20–22]. The wavelength of the Ti:S pump laser was measured by a Fizeau wavelength meter (Cluster Lambdameter LM-007). Since the purpose of this experiment was to detect the transition and study its population evolution, rather than the precise determination of the transition frequency, no precise calibration [19] was carried out on the reading of the wavelength meter or the Stokes-shifted light, and thus the precision on the transition frequency was limited to around ± 2 GHz which corresponds to a fractional precision of 1×10^{-5}. The spectral linewidth of the Stokes beam generated in this way is dependent on many parameters, such as the pressure of the H_2 gas and the intensity and focal position of the pump beam in the cell. No attempt was made to measure this linewidth.

Previous experiments [1, 2, 5] have shown that most of the antiprotons annihilate immediately after stopping in the target, while about 3% of them form the metastable $\overline{\mathrm{p}}\mathrm{He}^+$ atoms annihilating with an average lifetime of several microseconds. The resulting delayed annihilation time spectrum, i.e., the annihilation rate of antiprotons as a function of time elapsed after the atomic formation, was measured by the Cherenkov counter (Figure 2). The 1154.9 nm resonance was observed as a sharp peak in the time spectrum, since the laser induced the resonant annihilations (see above) within nanoseconds. Such a peak was observed at $t = 1.3$ μs (Figure 2).

Figure 3 shows the resonance profile of the 1154.9 nm transition. This was obtained by plotting the peak intensity in the time spectrum, averaged over 5 antiproton pulses, against the laser frequency. The data points in Figure 3 were fitted with two overlapping Lorentzian functions with a constant offset. The frequency interval between the two Lorentzian functions was fixed to the hyperfine splitting (2 GHz) which arises from the coupling between the electron spin and the antiproton orbital angular momentum [23]. This splitting, however, was small compared to the observed width of the resonance. We obtained a resonance centroid of $259\,577 \pm 2$ GHz. The experimental uncertainty is mostly due to the uncertainty on the laser wavelength and the statistical uncertainty of

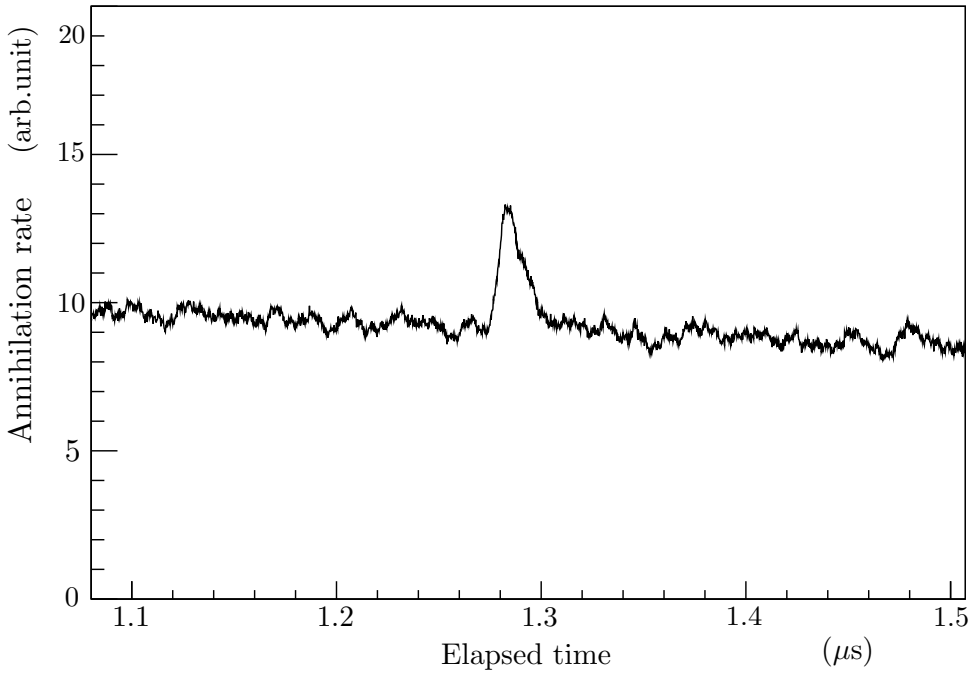

Figure 2. Delayed annihilation time spectrum of $\overline{\mathrm{p}}^4\mathrm{He}^+$, averaged over 5 antiproton pulses arriving at the experimental target. The laser-induced annihilation peak corresponding to the transition $(n, l) = (40, 36) \rightarrow (41, 35)$ is induced at $t = 1.3$ μs.

the data.

A three-body calculation [24] has determined the spin-independent transition frequency of this resonance as 259 591.042 GHz [25]. This differed from our experimental frequency which was measured in a helium target at an atomic density of $n_{\mathrm{He}} = 1.1 \times 10^{21}$ cm^{-3} by -14 GHz. Previous experiments [1, 2, 5] have shown that collisions between $\overline{\mathrm{p}}\mathrm{He}^+$ and normal helium atoms can shift the transition frequencies by many GHz. No attempt was made to measure this shift for this resonance. Chemical-physics calculations [26], however, predict a gradient $\beta = -11.3 \times 10^{-21}$ GHz cm^3 [27], which implies a shift $\Delta\nu_{\mathrm{col}} = \beta n_{\mathrm{He}} = -12$ GHz consummate with the above theory-experiment difference.

The full width at half maximum of the resonance profile was 16 ± 5 GHz. The experimental uncertainty includes contributions from the statistical uncertainty, and the systematic uncertainty arising from the choice of the fit function with a relatively large offset. We observed relatively strong signals in the spectral wings, far detuned from the resonance centroid. The reason for this unusual effect is not understood. One possibility is that a broadband light component in the laser beam was generated during

the wavelength conversion to 1154 nm in our simplified Raman gas cell [28]. Other possibilities include some collisional broadening effects.

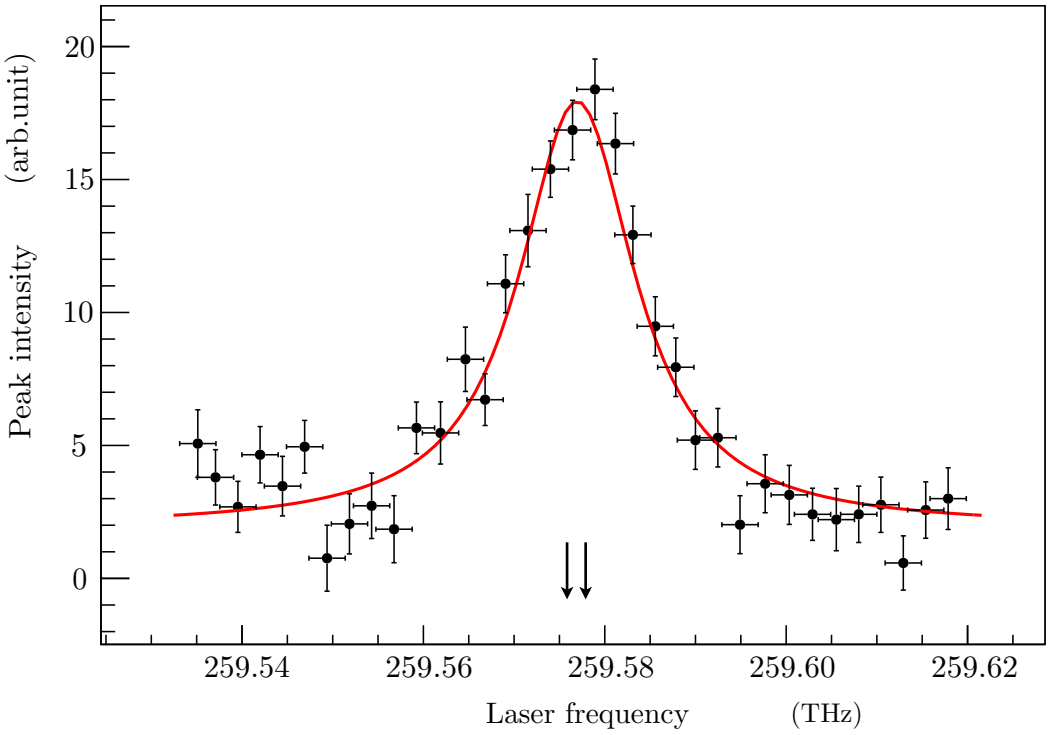

Figure 3. Resonance profile of the $\overline{\mathrm{p}}^4\mathrm{He}^+$ transition $(n, l) = (40, 36) \rightarrow (41, 35)$. The solid red curve indicates the best fit of two overlapping Lorentzian functions with a constant offset. The solid arrows indicate positions of the hyperfine lines.

The measured spectral linewidth is larger than the expected value 7 ± 2 GHz which was calculated by numerically solving the optical Bloch equation [7,29]. This simulation described laser-induced oscillations between the states $(40, 36)$ and $(41, 35)$. It included contributions from the Auger rate 5.9×10^7 s^{-1} of state (41,35) which was obtained from three-body calculations [24], and the collisional width of ~ 3 GHz estimated by chemical-physics calculations [26]. The spectral linewidth of the laser was tentatively assumed to be around ~ 1 GHz based on past works with similar lasers [21, 28, 30], but in fact may be larger (see above). The largest contribution to the resonance width arose from power broadening effects. The ± 2 GHz uncertainty in our simulated width is due to the uncertainty in our knowledge of the laser intensity in the experimental target. The reason for the difference between the measured and simulated linewidths is not understood. Some of the possibilities include an underestimation of collisional or power broadening effects, or the spectral linewidth of the laser. Past experiments [31] have shown that the measured and calculated Auger rates for many states agree with a

precision of $< 30\%$. In a small number of states [5, 31], however, the measured Auger width was much larger than some of the calculated values, due to the couplings with an electronically-excited $\bar{\mathrm{p}}\mathrm{He}^+$ state [32]. Other experiments have shown [5, 33] that some states become short-lived in collisions with other helium atoms, and similar effects could in principle increase the observed width of the resonance.

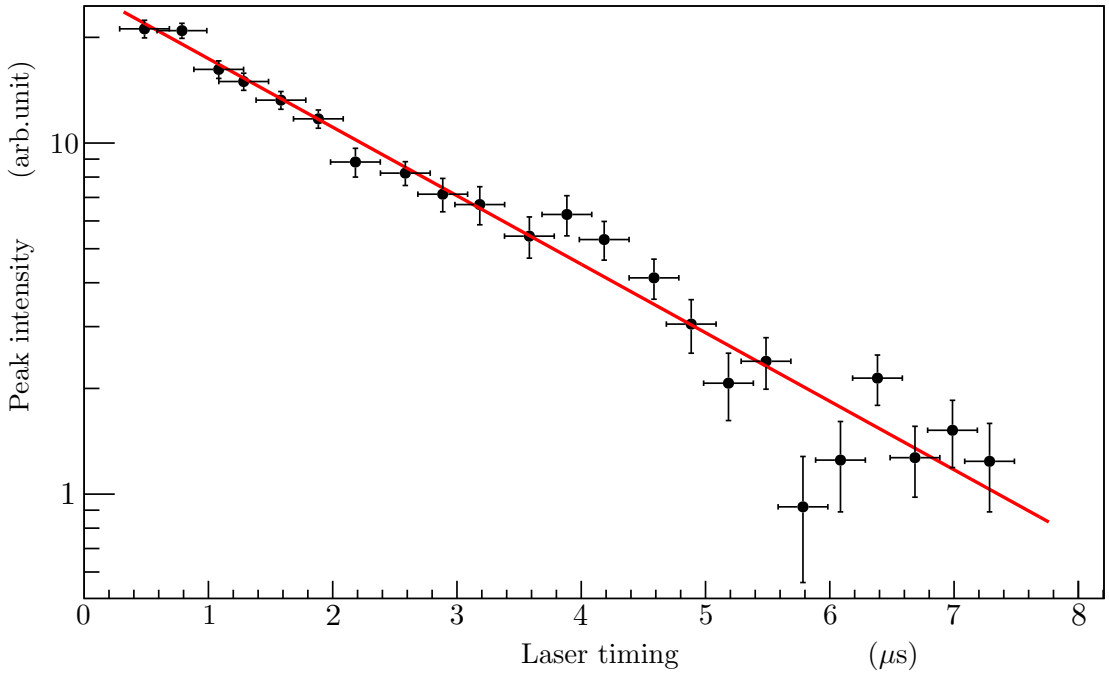

Figure 4. Time evolution of the resonance intensity $(n, l) = (40, 36) \rightarrow (41, 35)$. The laser frequency was fixed at the resonance centroid. The solid red line shows the best fit of a single exponential function.

Figure 4 shows the intensity of the laser-induced resonance spike, against the timing of the laser pulse which was varied between $t = 0.5$ and 8 μs. This corresponds to the time evolution of the population in the state $(40, 36)$, since the intensity of the spike at each t is proportional to the number of antiprotons occupying that state. The uncertainty of the spectral linewidth of the laser gives negligible effects on the measurement of the population evolution, since the laser frequency was fixed at the resonance centroid. The absolute number of $\bar{\mathrm{p}}\mathrm{He}^+$ that populate the state $(n, l) = (40, 36)$ can only be determined after carefully measuring various backgrounds and efficiencies [6, 7]. This was not done here, and so the y-axis in Figure 4 is given in arbitrary units. The solid line in Figure 4 indicates the best fit of a single exponential function. The population in the state (40,36) was found to decay with an effective lifetime of $\lambda_{\mathrm{exp}} = 0.45 \pm 0.04$ $\mu\mathrm{s}^{-1}$, in which the experimental uncertainty includes the statistical uncertainty and the systematic one due to the uncertainty in the arrival time of the 200-300-ns-long antiproton pulse from the AD. This value was in good agreement with the decay rate of 0.52 ± 0.18 $\mu\mathrm{s}^{-1}$ [7] which was indirectly estimated from previous studies on the lower-lying state $(39, 35)$. The radiative decay rate of the state $(40, 36)$

has been theoretically calculated as 0.55 μs^{-1} [34] and 0.47 μs^{-1} [25]. The former theoretical value was slightly larger than λ_{exp}, while the latter is in good agreement with λ_{exp}. This implies that the measured population evolution is well-represented by the intrinsic radiative decay rate of the state $(40, 36)$ and that the contributions to the population of this state due to the feeding from higher-lying states are small.

Previous experiments [6, 7] have indicated very little metastable populations in the $n \geq 41$ states. This was supported by our data in Figure 4. On the other hand, many theoretical calculations [35–42] have predicted that a considerable number of $\overline{p}He^+$ should be formed in the $n \geq 41$ states. In these calculations, the cross sections of antiprotons being captured into $\overline{p}He^+$ states were derived as a function of n- and l-values of the final states, using the classical trajectory Monte Carlo method [41] or a quantum mechanical calculation [42]. One possible reason for the apparent discrepancy between the experimental and theoretical results may be due to the fact that the populations are modified by collisions with helium atoms immediately after the atomic formation, which is not taken into account in the above calculations. The formed $\overline{p}He^+$ atoms are assumed to recoil with kinetic energies of several electronvolts, and undergo a rapid thermalization, i.e., they reach a thermal temperature within picoseconds by several collisions. Some theorists [43, 44] have suggested that most of the highly excited $\overline{p}He^+$ atoms are destroyed by collisions during the thermalization.

In summary, we have reported the observation of the transition $(n, l) = (40, 36) \rightarrow (41, 35)$ of $\overline{p}^4He^+$ at a wavelength of $\lambda = 1154.9$ nm. This demonstrated that some atoms are formed in the state $(40, 36)$, in agreement with previous experiments. The resonance centroid deviated from the theoretical transition frequency by -14 GHz. This was assumed to be due to collisional shifts which occurred at the relatively high target densities used in this experiment. The population of $\overline{p}He^+$ occupying the resonance parent state $(n, l) = (40, 36)$ was found to decay at an effective rate of 0.45 ± 0.04 μs^{-1}. This value is in good agreement with theoretical radiative rates for this state. This implies that few metastable atoms occupy states with $n \geq 41$ in the $v = 3$ cascade. In the future, we may measure this transition at lower target densities (e.g., $n_{He} \sim 10^{17}$ cm^{-3}) where collisional effects are small [45], or extend our laser resonance experiments to states with higher $n \geq 41$ principal quantum numbers.

Acknowledgments

We are grateful to the CERN BE department for their efforts in operating the AD. We would like to thank D. Bakalov, G. Ya. Korenman, V. I. Korobov, R. Pohl, and S. Sauge for theoretical and technical discussions. We are deeply indebted to the CERN cryogenics laboratory for technical assistance. This work was supported by the European Science Foundation (EURYI), the Deutsche Forschungsgemeinschaft (DFG), the European Research Council (ERC-StG), the Hungarian Research Fund (K103917), and the Grant-in-Aid for Specially Promoted Research (20002003) of MEXT, Japan.

References

[1] T. Yamazaki, N. Morita, R. S. Hayano, E. Widmann, and J. Eades, *Phys. Rep.* **366**, 183 (2002).
[2] R. S. Hayano, M. Hori, D. Horváth, and E. Widmann, *Rep. Prog. Phys.* **70**, 1995 (2007).
[3] M. Hori *et al.*, *Nature* **475**, 484 (2011).
[4] E. J. Salumbides, W. Ubachs, and V. I. Korobov, *arXiv*:1308.1711.
[5] M. Hori *et al.*, *Phys. Rev. Lett.* **87**, 093401 (2001).
[6] M. Hori *et al.*, *Phys. Rev. Lett.* **89**, 093401 (2002).
[7] M. Hori *et al.*, *Phys. Rev.* A **70**, 012504 (2004).
[8] J. S. Cohen, *Rep. Prog. Phys.* **67**, 1769 (2004).
[9] G. Ya. Korenman, *Hyperfine Interact.* **209**, 15 (2012).
[10] X. M. Tong and N. Toshima, *Phys. Rev.* A **85**, 032709 (2012).
[11] K. Sakimoto, *Phys. Rev.* A **82**, 012501 (2010).
[12] J. S. Cohen, *Phys. Rev.* A **65**, 052714 (2002).
[13] J. S. Briggs, P. T. Greenland, and E. A. Solv'ev, *Hyperfine Interact.* **119**, 235 (1999).
[14] E. Fermi and E. Teller, *Phys. Rev.* **72**, 399 (1947).
[15] A. S. Wightman, *Phys. Rev.* **77**, 521 (1950).
[16] A. Sótér, D. Barna, and M. Hori, *in preparation.*
[17] M. Hori, *Rev. Sci. Instrum.* **76**, 113303 (2005).
[18] M. Hori *et al.*, *Nucl. Instrum. Methods Phys. Res.* A **496**, 102 (2003).
[19] M. Hori and A. Dax, *Opt. Lett.* **8**, 1273 (2009).
[20] D. E. Jennings, A. Weber, J. W. Brault, *Appl. Opt.* **25**, 284 (1986).
[21] W. K. Bischel and M. J. Dyer, *Phys. Rev.* A **33**, 3113 (1986).
[22] M. J. Dyer and W. K. Bischel, *Phys. Rev.* A **44**, 3138 (1991).
[23] D. Bakalov and V. I. Korobov, *Phys. Rev.* A **57**, 1662 (1998).
[24] V. I. Korobov, *Phys. Rev.* A **77**, 042506 (2008).
[25] V. I. Korobov, *private communication.*
[26] D. Bakalov *et al.*, *Phys. Rev. Lett.* **84**, 2350 (2000).
[27] D. Bakalov, *private communication.*
[28] D. V. Guerra and R. B. Kay, *J. Phys. B : At. Mol. Opt. Phys.* **26**, 3975 (1993).
[29] M. Hori and V. I. Korobov, *Phys. Rev.* A **81**, 062508 (2010).
[30] B. E. Grossmann *et al.*, *Appl. Opt.* **26**, 1617 (1987).
[31] H. Yamaguchi *et al.*, *Phys. Rev.* A **66**, 022504 (2002).
[32] O. I. Kartavtsev *et al.*, *Phys. Rev.* A **61**, 062507 (2000); **61**, 019901(E) (2000).
[33] M. Hori *et al.*, Phys. Rev. A **57**, 1698 (1998); **58**, 1612(E) (1998).
[34] P. T. Greenland and R. Thürwächter, *Hyperfine Interact.* **76**, 355 (1993).
[35] K. Ohtsuki, *private communication.*
[36] G. Ya. Korenman, *Hyperfine Interact.* **101-102**, 81 (1996); *Nucl. Phys.* **A692**, 145c (2001).
[37] J. S. Cohen, R. L. Martin, and W. R. Wadt, *Phys. Rev.* A **27**, 1821 (1983).
[38] V. K. Dolinov *et al.*, *Muon Cat. Fusion* **4**, 169 (1989).
[39] W. A. Beck, L. Wilets, and M. A. Alberg, *Phys. Rev.* A **48**, 2779 (1993); *private communication.*
[40] J. S. Cohen, *Phys. Rev.* A **62**, 022512 (2000).
[41] K. Tőkési, B. Juhász, and J. Burgdörfer, *J. Phys. B : At. Mol. Opt. Phys.* **38**, S401 (2005).
[42] J. Révai and N. Shevchenko, *Eur. Phys. J. D* **37**, 83 (2006).
[43] G. Ya. Korenman, *Phys. At. Nucl.* **59**, 1665 (1996).
[44] S. Sauge and P. Valiron, *Chem. Phys.* **265**, 47 (2001).
[45] M. Hori *et al.*, *Phys. Rev. Lett.* **91**, 123401 (2003).